

Piezoelectric Actuators Characterization for Simultaneous Force and Displacement Self-Sensing by detecting Impedance

BAFUMBA LISELI, Joël * ZARIF MANSOUR, Sepehr **
SEETHALER, Rudolf ** AGNUS, Joël * LUTZ, Philippe *
RAKOTONDRABE, Micky ***

* *FEMTO-ST Institute, Université de Bourgogne Franche-Comté,
Besançon, France,*

** *School of Engineering, University of British Columbia, Kelowna, BC,
Canada V1V1V7,*

*** *Laboratoire Génie de Production (LGP),
National Engineering School of Tarbes (ENIT), France,
e-mail of corresponding author: micky.rakotondrabe@enit.fr.*

Abstract: This paper introduces a new Self-Sensing Actuation approach for simultaneous estimation of external loads and Piezoelectric Actuator (PEA) displacement at a frequency where the PEA's impedance change presents good sensitivity to both electrical and mechanical excitations. Experiments are conducted for static operations to support these claims and to help demonstrate the dependence of the PEA's mechanical and electrical properties on external excitations: mechanical stresses with a low preload (less than the recommended 15 MPa for dynamic operations) and electric fields.

Keywords: Piezoelectric actuator, Force and Displacement Self-Sensing Actuation, Impedance measurement.

1. INTRODUCTION

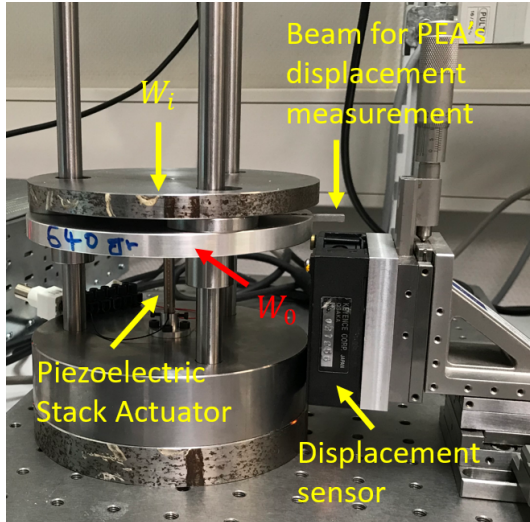
The world is witnessing an increasing growth of miniaturization of products. This miniaturization is accompanied by a need to perform not only micromachining but also microassembly and micromanipulation tasks. These tasks require precise positioning with very high accuracy, generally better than the micron. It should also be noted that microscopic objects are generally fragile (objects of small dimensions that are often made of special materials) so that the forces exerted during their handling must be adapted and controlled. To reach such resolution and accuracy precise positioning systems are used. These systems generally consists of three subsystems: (1) A mechanism that is driven, (2) Actuators that drive the mechanism and govern the limits of the best possible performance, and (3) Sensors that track, monitor and report on the mechanism output performance.

The high resolution, high bandwidth, small size and high force density of piezoelectric materials make them a good contender as actuators when developing systems acting at the nanoscale. In addition to their actuation role, piezoelectric transducers are also widely utilized as high sensitivity strain sensors [Yong et al. 2013] and force sensing devices in nanopositioning systems [Shen et al.

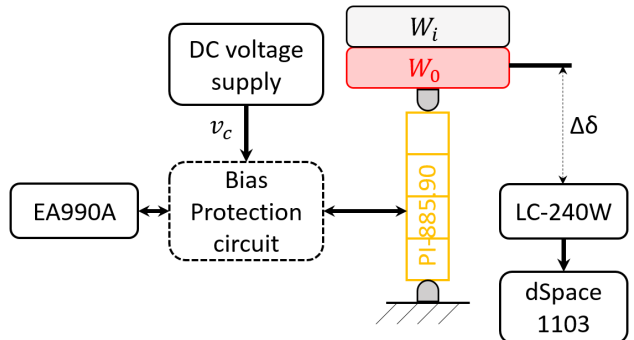
2004]. In counterpart, PEAs are known to exhibit hysteresis and creep nonlinearities between input voltages and the generated displacement. Even if they have nanometric resolution, the final accuracy and even the stability of the tasks they perform are strongly compromised by these nonlinearities. These nonlinearities should therefore be attenuated or removed by mandatorily implementing controllers for the PEA [Devasia et al. 2007].

Different control schemes for positioning control of PEAs have been introduced. Feedforward control schemes that depend on the accuracy of the PEA's model [Rakotondrabe 2017], feedback control schemes that rely entirely on sensors precision [Zhang and Yan 2017], and charge amplifiers whose efficiency depends on its hardware complexity [Fleming and Leang 2008]. For further performance improvement, combined control schemes such as feedforward-feedback voltage control scheme [Omar Aljanaideh and Janaideh 2017] and integrated voltage-charge control strategy [Clayton et al. 2008] were introduced to overcome limitations imposed by the need to balance a high-bandwidth precision positioning with robust closed-loop stability in the presence of unmodeled dynamics, uncertainties, and disturbances. The integrated voltage-charge control strategy permits a control of a linearized PEA but remains a feedforward scheme that lacks robustness against external disturbances and is likely to induce a loss in accuracy during the positioning. Feedforward-feedback control scheme, if properly designed, can be robust to both internal uncertainties in the modeling and external disturbances; however, the feedback

* This work has been supported by the EIPHI Graduate school (Contract ANR-17-EURE-0002). This work was also partially supported by the national CODE-Track project (ANR-17-CE05-0014-01) and by the CNRS BIOMIMBOT project.



(a) Photography of the experimentation procedure.



(b) Schematic block diagram of the experiment.

Fig. 1. Test setup.

branch requires sensors. Unfortunately, accurate sensors are bulky and are difficult to downscaling manipulation systems.

Soft-sensors aid in solving the problem created by the unavailability of embeddable and precise sensors by providing a software backup for it. Soft-sensors are inferential estimators based on control theory that provides an estimate of the internal state of a given real system, from available measurements thereof. Software sensors use more suitable hardware sensors that do not directly measure the physical signal of interest; however, associated with an algorithm, they make it possible to reconstruct the signal of interest. The Self-Sensing Actuation (SSA) is the PEA's soft-sensor implementation.

The principle of SSA is defined by the capability of deriving the physical state of a PEA (displacement, perceived force, \dots) without the use of external sensors to directly measure thereof, but rather by estimating it from the measurement of less intrusive and cheaper physical signals produced by the PEA itself (throughout current, voltage drop, \dots). The main advantage of SSA is the reduction of space occupancy, allowing for better miniaturization of micro-manipulation/micro-assembly cells.

SSA can be classified into two approaches: (1) SSA based on the piezoelectric direct effect which consists on a dual dielectric feedthrough cancellation to recover the signal arising from the PEA's strain. It is achieved by using a capacitance bridge where one represents the PEA either as a strain-dependent voltage source (*Voltage-based SSA*) [Rakotondrabe 2013] or with an antiparallel circuit when one chooses to represent the PEA as a strain-dependent charge source (*Charge-based SSA*) [Pillai et al. 2018]. (2) SSA based on the PEA's change of electrical properties, that is, by measuring the changing relative permittivity [Saigusa and Morita 2015], or capacitance [Mansour and Seethaler 2018] to estimate the PEA's displacement and/or perceived force. SSA based on the piezoelectric direct effect demands a tedious continual tuning in order to discriminate the signal that is related to the PEA's strain from the

TABLE I. Reference values for PI-885.90 from PICeramics

| | |
|----------------------------------|-----------------------------------|
| Dimensions $a \times b \times l$ | 5 mm \times 5 mm \times 36 mm |
| h_p (Ceramic layer thickness) | 60 μ m |
| k (stiffness) | 25 N/ μ m |
| Operating range | 0 to 100 V |
| Max. no load displacement | 38 μ m@100 V |
| Max. clamped force | 950 N @ 120 V |
| C (capacitance) | $3.1 \pm 20\%$ (μ F) @1 KHz |
| Resonant frequency | 40 KHz |

dielectric signal and the noisy environmental conductive materials or outer metal parts such as electrical wires [Moheimani 2003] and will not be considered in this paper. This paper is dedicated to the SSA based on the PEA's change of electrical properties, as it has demonstrated the most potential in recent researches and is less prone to error due to its surrounding.

While one already knows that applying an electric field and/or an external load induces a strain in the PEA, recent works have shown that the PEA's impedance is also affected by electric field application [Liseli et al. 2018] and external loads [Mansour and Seethaler 2018]. The current paper is devoted to: (1) introducing a design that allows to independently apply electric field and mechanical loads and to study the effect of both on the PEA's impedance and strain, (2) establishing a link between impedance, displacement and perceived force, and (3) suggesting a new approach for simultaneous force and displacement Self-Sensing Actuation and control system.

The remainder of the article is organized as follows. In section II, the test setup is presented along with results to highlight the PEA's mechanical and electrical properties dependence to external excitations. In section III, a displacement-force-voltage map and impedance-force-voltage map from the test setup is generated. Experimental results are particularly discussed and a displacement and force control structure is suggested. Finally, conclusions are provided in section IV.

2. PIEZOELECTRIC EFFECT : DYNAMIC PROPERTIES

The test setup (see figure 1) to be used comprises:

- A dSPACE-board (DS1103) and a computer for the data acquisition and observer implementation;
- An impedance Analyzer EA990A. Operating characteristics: OSC level 500 mV, frequency range [20 Hz, 20 MHz];
- A piezoelectric stack actuator PI-885.90 from PICE-ramic (see specifications in TABLE I);
- A displacement sensor KEYENCE LC-2400W with some tens of nanometers of resolution and an accuracy of 100 nm;
- A preload mass $W_0 = 0.64$ Kg, and several masses, $W_i |_{i=1, \dots, 11} = 1.15$ Kg $\pm 5\%$;
- A DC voltage supply CN7 B D up to 200 V;
- An external DC voltage bias protection circuit for a DC (from 0 to 100 V) biased impedance measurement [Haruta 2000].

Dahiya et al. [Dahiya and Valle 2012] theoretically demonstrated that due to the piezoelectric phenomenon (direct and reverse effect), piezoelectric's stiffness and dielectric constant are not fixed but, rather depends on the operating conditions: applied voltage and/or external loads. Measurements realized with the abovementioned experimental setup are intended to validate that claim and will serve as an introduction to the notion of dependence between PEA's strain, impedance, and perceived force.

2.1 The effect of external force on the PEA's impedance and elastic constant

With the control input voltage v_c held at 0 V, let us vary the weights W_i in the poling direction of the PiezoStack and at the same time measure the variation of the impedance $Z_i(|Z_i|/\Phi_i)$ and the resulting displacement $\Delta\delta_i$. From the known weights and the resulting displacement, one can deduce the PEA's stiffness:

$$k_{33_n}^E = \frac{W_n}{\Delta\delta_n} \quad (1)$$

where, $W_n = \sum_{i=0}^n W_i$ and $\Delta\delta_n$ is the displacement caused by W_n .

Figure 2a depicts how the PEAs stiffness is changing in relation to the mechanical stress applied upon it. All the conducted measurements were realized with a preload lower than the recommended preload for dynamic operations by the manufacturer. This likely has led to a more nonlinear correlation between applied external forces and displacement. Eq. 2 gives a model that fits the experimental data using the Matlab fitting tool.

$$k_{33}^E(T_3) = 1.58 \times 10^6 e^{-1.1 \times 10^{-6} T_3} + 7.06 \times 10^5 e^{-4.43 \times 10^{-8} T_3} \quad (2)$$

where, $T_{3_n} = \frac{W_n}{A}$ is the stress applied in the poling direction. $A = a \cdot b$ is the actuator cross-sectional area (see Figure 5).

Figure 3 illustrates the PEA's impedance variation as a function of the impedance analyzer sweep frequency f and the applied weights. From the impedance phase graph $\Phi(W, f)$ one realizes that the PEA goes from a

capacitor ($\Phi(W, f \leq 10^4 \text{ Hz}) \approx -90^\circ$) to an inductor ($\Phi(W, f \geq 10^6 \text{ Hz}) \approx 90^\circ$). Therefore, the model to be adopted to characterize the PEA electrical behavior is frequency dependent. From the impedance gain graph ($|Z(W, f)|$) one notices that the gain $|Z(W, f)|$ decreases exponentially and the higher the frequency the less sensitive to the applied weight $|Z(W, f)|$ becomes. An identical behavior is observed when varying v_c , as it can be noted in figure 4. Since one is interested in the PEA's impedance sensitivity to the deformation thereof (a deformation that may be caused by W_i and/or v_c), $f_r = 25$ Hz is chosen to be the frequency of interest. At this frequency, the impedance phase is quasi-constant and the PEA behaves essentially as a capacitor independently of either the applied weight or input voltage. The deformation caused by applied weights and input voltages is perceived through the impedance magnitude variation. The Pearson correlation coefficient between W and $|Z(W, 25 \text{ Hz})|$ is $r_{(W, |Z(W, 25 \text{ Hz})|)} = -0.8717$. This indicates that there is a weak linear correlation between these two variables. However, this does not exclude the possibility of a nonlinear relationship between W and $|Z(W, 25 \text{ Hz})|$. The applied weight W and the resulting PEA's tip displacement $\Delta\delta$, on the other hand, have a strong linear correlation with $r_{(W, \Delta\delta)} = -0.9968$. This suggests that a linear relationship may be established between these two variables.

2.2 The effect of applied electric field on the PEA's impedance and dielectric constant

For this part of the experiments, only the preload W_0 is held upon the piezostack while one varies v_c and measures the variation of the impedance and the resulting PEA's displacement. The applied voltage will cause the deformation of the PEA and thus the modification of its electrical properties. For $f_r = 25$ Hz, the PEA is modeled as a capacitor which makes it possible to relate the PEA's tip displacement $\Delta\delta$ to the variation of its capacitance C . The variable capacitance C resulting from the PEA's deformation can be calculated either from the measured impedance at a fixed frequency (in this case, $f_r = 25$ Hz) or as for a piezostack actuator with a known number of ceramic layers n , that is:

$$C = -\frac{1}{2\pi f_r (|Z(f_r)| \sin \Phi(f_r))} = n \varepsilon_{33}^T \frac{A}{h_p + \Delta\delta} \quad (3)$$

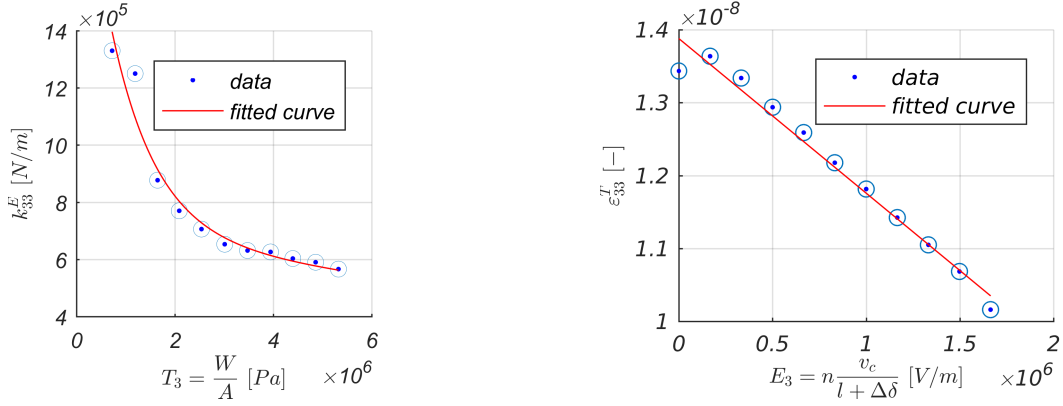
where, $A = a \cdot b$ is the actuator cross-sectional area which deformation is supposed neglected ($\Delta A_i \ll A_i$, $A_i = A \forall i$), and $\varepsilon_{33}^T = \frac{\varepsilon}{\varepsilon_0}$ the relative permittivity ($\varepsilon_0 = 8.854 \times 10^{-12}$ F/m is the vacuum permittivity).

At a fixed actuator length l (see figure 5), the following holds true when $n \approx \frac{l}{h_p}$:

$$C = l \varepsilon_{33}^T \frac{A}{h_p^2} \quad (4)$$

From the impedance measurement and Eq. 4 one can describe ε_{33}^T as a function of the applied electric field E_3 for $f_r = 25$ Hz (see figure 2b). The relative permittivity ε_{33}^T is deduced from the varying PEA's capacitance as follows:

$$\varepsilon_{33}^T = \frac{C h_p^2}{(l + \Delta\delta) A} \quad (5)$$



(a) The dependence of the PEA's stiffness on the applied (b) The dependence of the PEA's dielectric constant on the mechanical stress. applied electric field.

Fig. 2. The dependence of PEA's electrical and mechanical properties to external excitations.

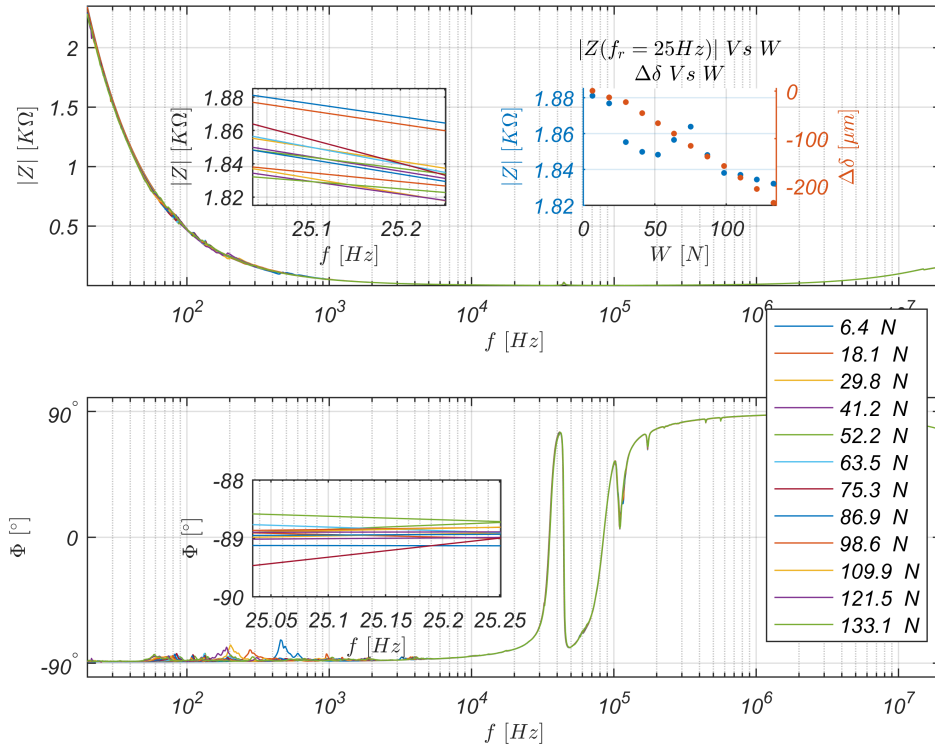


Fig. 3. PEA's impedance as a function of the impedance analyzer sweep frequency and applied weights.

Eq. 6 gives the linear model that fits the experimental data using the Matlab fitting tool.

$$\varepsilon_{33}^T(E_3(f_r)) = 1.388 \times 10^{-8} - 2.121 \times 10^{-15} E_3(f_r) \quad (6)$$

From Eq. 2 and Eq. 6, the constitutive equation of piezoelectricity for a piezostack can be rewritten as:

$$\begin{cases} S_3 = s_{33}^E(T_3)T_3 + d_{33}E_3 \\ D_3 = d_{33}T_3 + \varepsilon_{33}^T(E_3(f_r))E_3 \end{cases} \quad (7)$$

where, $s_{33}^E = \frac{1}{k_{33}^E}$ is the elastic compliance at constant electric field E , ε_{33}^T is the dielectric constant under constant stress T , d_{33} is the piezoelectric constant, S_3 is the mechan-

ical strain, and D_3 is the resulting electric displacement. All these elements are in the poling direction.

Unlike the W and $|Z(W, 25\text{Hz})|$ correlation, the impedance's gain change induced by v_c , $|Z(v_c, 25\text{Hz})|$, has a strong linear correlation with both the induced PEA's displacement $\Delta\delta$ and v_c . Again using the Pearson correlation coefficient one obtains $r(|Z(v_c, 25\text{Hz})|, \Delta\delta) = 0.9807$ and $r(|Z(v_c, 25\text{Hz})|, v_c) = 0.9987$. That is, a linear relationship is sufficient to estimate the resulting displacement from the impedance gain.

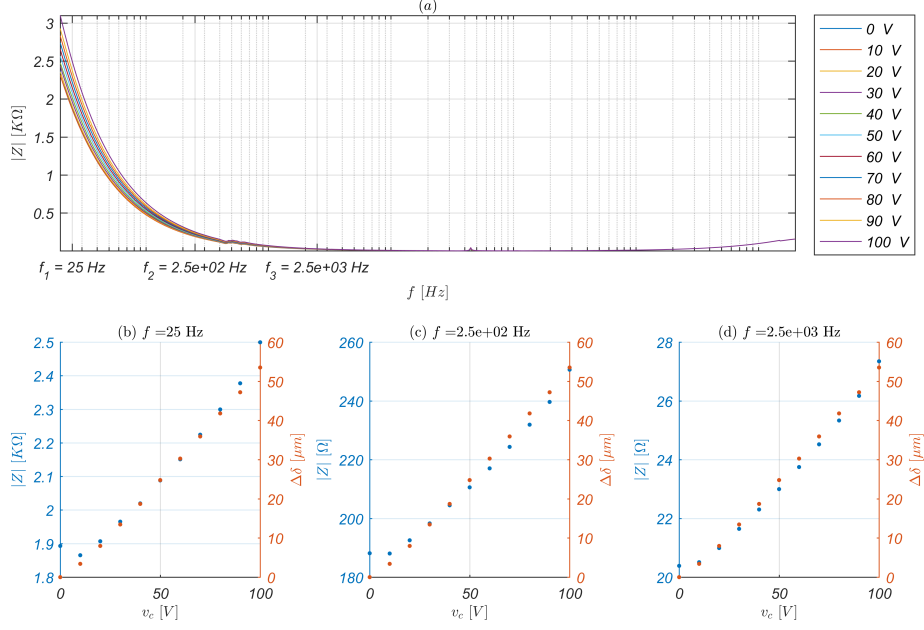


Fig. 4. PEA's impedance as a function of the impedance analyzer sweep frequency and control input voltage.

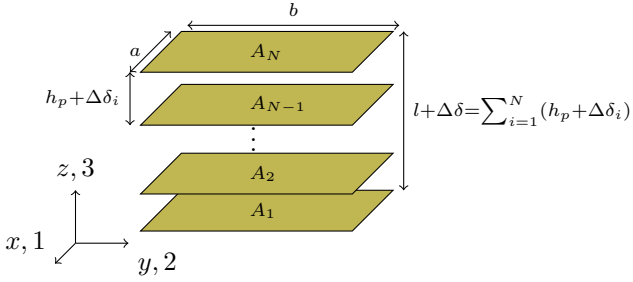


Fig. 5. Simplified representation of electrodes' arrangement of a Piezoelectric Stacks.

3. THE PROPOSED SELF-SENSING TECHNIQUES FOR SIMULTANEOUS EXTERNAL LOADS AND DISPLACEMENT ESTIMATION

Instead of independently varying W_n and v_c , they vary simultaneously in this part, so that one can observe their joint impact on the PEA's tip displacement and impedance variation. This joint impact can be represented as maps (see figure 6(a) for the impedance magnitude map, and figure 6(b) for the displacement map). These maps are created from new independent experiments with varying input voltages and weights and not by extrapolation from the data in the previous section. They are created off-line to characterize the PEA electrical and mechanical behaviors for an online simultaneous estimation of the PEA's strain and perceived external force. It should also be noted that these data were created from continuously increasing input voltage rather than from an increasing and decreasing voltages, that would likely produce hysteresis loops between the displacement and input voltage. But since, the displacement - impedance relationship is linear [Islam et al. 2011], no hysteresis loop

is expected from the estimation of the PEA's strain from impedance measurement.

As abovementioned, the SSA is an inferential estimator that provides an estimate of the PEA's state, PEA's strain and perceived force in this case, from measurements of the input (v_c) and output $Z(25 \text{ Hz}, W, v_c)$. The phase is almost constant and indicates that the PEA behaves as a capacitor independently of both the weights and the input voltage at this frequency, i.e., $\Phi(25 \text{ Hz}, W, v_c) \approx -90^\circ$. Therefore, one only has the measured impedance magnitude $|Z(25 \text{ Hz}, W, v_c)|$ and the known applied voltage v_c for the estimation. Two possibilities for the estimator:

- A *look-up table method* where the impedance and displacement maps are simultaneously consulted as table for a given v_{c_j} and measured $|Z_{i,j}(25 \text{ Hz}, W_i, v_{c_j})|$. For non-tabulated values of v_{c_j} and $|Z_{i,j}(25 \text{ Hz}, W_i, v_{c_j})|$, the PEA's strain and perceived force are estimated through interpolation or extrapolation.

- Two relationships:

$$W = f_1(v_c, |Z(f = 25 \text{ Hz})|) \quad (8)$$

$$\Delta\delta = f_2(v_c, |Z(f = 25 \text{ Hz})|) \quad (9)$$

where, f_1 and f_2 are functions found by fitting the PEA's displacement and impedance's magnitude maps using the Matlab fitting tool.

4. CONCLUSION

A new SSA-based observer to estimate a piezostack's strain, and the external force applied thereto is suggested in this paper. The suggested approach uses a mapping of resulting electric (impedance) and mechanical (displacement) changes from external excitations (electric field and mechanical stress) to estimate the PEA's perceived force and/or strain. From the test setup, the impedance

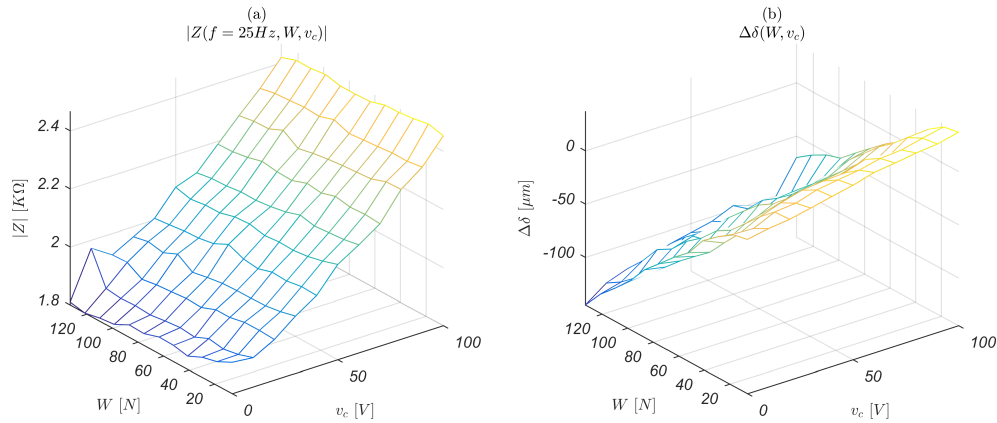


Fig. 6. Impedance and Displacement maps.

magnitude and displacement maps are generated. These maps can be used either through a *look-up table* method or by fitting functions to retrieve the information on PEA's strain and perceived force from impedance measurement and the knowledge of input voltage.

All the conducted measurements were performed with a preload less than the manufacturer recommended preload for dynamic operations. This likely led to a more non-linear correlation between applied external forces and displacement. The next steps are (1) the design of a real-time PEA's impedance variation measurement scheme, which will make possible an online estimation of the displacement thereof and the force applied thereto, and (2) the extension of the approach to a multi-degrees of freedom SSA-based observer for a multi-axis' displacement and contact force control.

REFERENCES

- Clayton, G., Tien, S., Fleming, A., Moheimani, S., and Devasia, S. (2008). Inverse-feedforward of charge-controlled piezopositioners. *Mechatronics*, 18(5-6), 273–281.
- Dahiya, R.S. and Valle, M. (2012). *Robotic tactile sensing: technologies and system*. Springer Science & Business Media.
- Devasia, S., Eleftheriou, E., and Moheimani, S.R. (2007). A survey of control issues in nanopositioning. *IEEE Transactions on Control Systems Technology*, 15(5), 802–823.
- Fleming, A. and Leang, K. (2008). Charge drives for scanning probe microscope positioning stages. *Ultra-microscopy*, 108(12), 1551–1557.
- Haruta, H. (2000). *The impedance measurement handbook: a guide to measurement technology and techniques*. Agilent Technologies.
- Islam, M., Seethaler, R., and Mumford, D. (2011). Hysteresis independent on-line capacitance measurement for piezoelectric stack actuators. In *Electrical and Computer Engineering (CCECE), 2011 24th Canadian Conference on*, 001149–001153. IEEE.
- Liseli, J.B., Agnus, J., Lutz, P., and Rakotondrabe, M. (2018). Self-sensing method considering the dynamic impedance of piezoelectric based actuators for ultralow frequency. *IEEE Robotics and Automation Letters*, 3(2), 1049–1055.
- Mansour, S.Z. and Seethaler, R. (2018). Simultaneous quasi-static displacement and force self-sensing of piezoelectric actuators by detecting impedance. *Sensors and Actuators A: Physical*, 274, 272–277.
- Moheimani, S.R. (2003). A survey of recent innovations in vibration damping and control using shunted piezoelectric transducers. *IEEE transactions on control systems technology*, 11(4), 482–494.
- Omar Aljanaideh, Micky Rakotondrabe, I.A.D. and Janaideh, M.A. (2017). Internal model-based feedback control design for inversion-free feedforward rate-dependent hysteresis compensation of piezoelectric cantilevered actuator. *Control Engineering Practice*, 72, 29–41.
- Pillai, M.A., Ebenezer, D., and Deenadayalan, E. (2018). Design and optimization of piezoelectric unimorph beams with distributed excitation. *The Journal of the Acoustical Society of America*, 143(5), 2685–2696.
- Rakotondrabe, M. (2013). Combining self-sensing with an unknown-input-observer to estimate the displacement, the force and the state in piezoelectric cantilevered actuator. *American Control Conference*, 4523–4530.
- Rakotondrabe, M. (2017). Multivariable classical prandtl-ishlinskii hysteresis modeling and compensation and sensorless control of a nonlinear 2-dof piezoactuator. *Nonlinear Dynamics*, DOI: 10.1007/s11071-017-3466-5.
- Saigusa, K. and Morita, T. (2015). Self-sensing control of piezoelectric positioning stage by detecting permittivity. *Sensors and Actuators A: Physical*, 226, 76–80.
- Shen, Y., Xi, N., Wejinya, U.C., and Li, W.J. (2004). High sensitivity 2-d force sensor for assembly of surface mems devices. In *Intelligent Robots and Systems, 2004.(IROS 2004). Proceedings. 2004 IEEE/RSJ International Conference on*, volume 4, 3363–3368. IEEE.
- Yong, Y.K., Fleming, A.J., and Moheimani, S. (2013). A novel piezoelectric strain sensor for simultaneous damping and tracking control of a high-speed nanopositioner. *IEEE/ASME Transactions on Mechatronics*, 18(3), 1113–1121.
- Zhang, Y. and Yan, P. (2017). Modeling, identification and compensation of hysteresis nonlinearity for a piezoelectric nano-manipulator. *Journal of Intelligent Material Systems and Structures*, 28(7), 907–922.